Proceedings of the 5th WSEAS International Conference on Applications of Electrical Engineering, Prague, Czech Republic, March 12-14, 2006 (pp96-101)

Terminal Models for Switching Overvoltage Studies in Electrical Machines

J. L. Guardado, V. Venegas, E. Melgoza
ITM P.O. Box 262
Postgraduate Program in Electrical Engineering
Morelia, Mich. México

Abstract- In this paper, terminal models for high voltage machine windings are developed. The models are useful for simulating transient overvoltages due to switching operations on industrial installations. The models are based on network synthesis of the winding terminal impedance. The process of synthesis is carried out by taking into account the winding resonant frequencies. The computer models arte validated by a comparison of measurements and the calculated transient overvoltages and winding impedances in a high voltage motor.

Keywords- Machine winding, electrical parameters, network synthesis, terminal impedance, switching transients.

1. Introduction[1].

For modeling electrical machine windings during switching transient several computer models have been developed, mainly in the frequency domain [1,2,3,4,5]. However, the use of these models on industrial installations is limited because they are too detailed to be used in a context of several buses, circuit breakers, motors and cable connections.
In order to simplify machine winding modelling during transient conditions it is desirable to have a terminal representation for the machine winding. This representation facilitates the use of computer programs for transient analysis like the Alternative Transient Program (ATP).
The aim of this work is to develop time domain terminal models for electrical machine windings. The first step in the development of the models is the calculation of the machine winding electrical parameters using the finite element method. Further, electrical circuits representing the winding terminal impedance are obtained by using network synthesis. Then, the electrical circuit obtained is used in the ATP program for switching transient calculations. The results of this study are useful for simulating switching transients on industrial installations involving electrical machine windings.

[1] The present work was supported by COSNET and CONACYT of México.

2. Calculation of Electrical Parameters.

A complete description of the electrical parameters calculation is given in [6]. A brief summary of the method is presented in this section.
A single coil is the basic element for the calculation of winding parameters. Each coil can be divided in two sections: the slot and the overhang region; therefore the inductance, resistance and capacitance are calculated for both sections.
The machine inductance and resistance depend of the magnetic flux penetration in the conductor regions (cooper and iron). In a conductor material this penetration can be estimated by:

$$\delta = \sqrt{\frac{2}{\omega\sigma\mu}} \tag{1}$$

where T is the angular frequency, Φ the conductivity and μ the permitivity of the medium. Equation (1) is used to estimate the magnetic flux penetration as a function of frequency.
For the adequate development of finite element models it is necessary to take into account the value of ∗ for estimating the size of elements in the mesh that represents conductor regions. Equation (1) is also used to estimate iron mesh dimensions for the development of models.

2.1. Inductance Calculation.

The inductance in the slot section is calculated using the stored magnetic energy over the region of analysis. This energy per unit length is given by [6]:

$$W_m = \frac{1}{2\mu} \int_s \boldsymbol{B}^2 \, ds \qquad (2)$$

where $\boldsymbol{B}$ is the magnetic flux density. The self inductance in the slot section is computed at different frequencies from the stored energy and the total current circulating through the coil conductors:

$$L_{slot} = \frac{2W_m}{I^2} \qquad (3)$$

In the overhang section, the inductance $L_{overhang}$ is calculated using an axisimetric model by approximating the end winding to one half of a toroid. The mutual inductances between end winding coils are expressed as a function of the coil geometrical position in the stator and the coil self inductance $L_{overhang}$ as proposed in [6].
Figures 1 and 2 show the magnetic flux distribution at 200 kHz and 1 MHz respectively, for a single coil located in a stator slot of the machine under study. It is evident that a major portion of the flux is confined to the coil insulation at higher frequencies, as a result of the minor depth of penetration into the iron core.

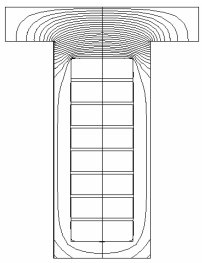

Fig. 1. Magnetic flux distribution at 200 kHz

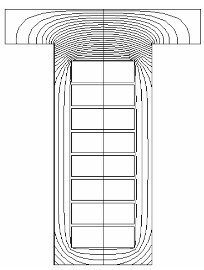

Fig. 2. Magnetic flux distribution at 1 MHz

Figure 3 shows the inductance values measured and calculated for one coil in the frequency range from 0 to 200 kHz. From Figure 3 it can be concluded that the computer model is capable of calculating the coil inductance with a reasonably degree of accuracy. Also, it can be observed that the inductance tends to decrease when the frequency increases. This can be explained by the fact that for greater frequencies, the flux penetration into the cooper and iron materials is limited by Eddy currents.

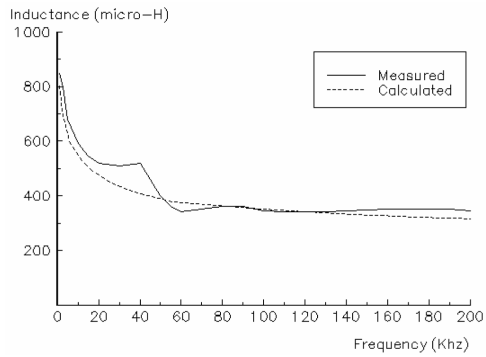

Fig. 3. Coil inductance measured and calculated.

2.2. Resistance Calculation

The power losses can be calculated with:

$$P = \frac{1}{2\sigma} \int_s \boldsymbol{J} \cdot \boldsymbol{J}^* \, ds \qquad (3)$$

and the coil series resistance R by the well known expression:

$$R = \frac{P}{I^2} \qquad (4)$$

where I is the total current in the conductor region. For the iron region, this is the current induced by the varying magnetic field.
Figure 4 shows the series resistance measured and calculated in the frequency range from 0 to 200 kHz for a single coil located in the stator of motor under study. From Figure 4 it can be concluded that the computer model calculates results which has a good approximation with those measured.

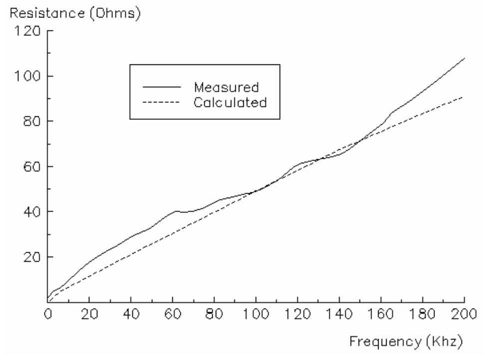

Fig. 4. Resistance measured and calculated

Also, it is observed that series resistance tends to increase for greater frequencies. This is due to the fact that the skin effect confines currents to small sections of the conductor material, increasing the effective resistance.

2.3. Capacitance Calculation

The electrostatic field energy, given by:

$$W_e = \frac{1}{2}\int_s \varepsilon \boldsymbol{E}^2 \, ds \,, \qquad (5)$$

is the basis for calculating the winding capacitance. The analysis of the electrostatic field by the Finite Element Method allows the determination of this energy.

Self-capacitance of the *i-th* winding conductor is obtained by considering that its applied electrical potential is V_i while the potential of other conductors is zero, such that:

$$C_{ii} = \frac{2W_e}{V_i^2} \qquad (6)$$

Mutual-capacitance is obtained with:

$$W_{ij} = \frac{1}{2}C_{ii}V_i^2 + \frac{1}{2}C_{jj}V_j^2 + C_{ij}V_iV_j \qquad (7)$$

by assuming that electrical potentials V_i and V_j are applied to the *i-th* and *j-th* conductors, while all other conductors are at zero potential.

Measured and computed results for the capacitance of a single coil of the induction motor is shown in Fig. 5. Again, the calculated results are in good agreement with the measurements for the analyzed frequency range.

In general, the calculated resistance, inductance and capacitance have a good agreement with the measurements in the motor coils considered in this study, except for the frequencies close to the main resonant frequency of the coil. For these frequencies there is a distortion of measured results, which starts approximately in 160 kHz. That is the reason why the computed parameters are less accurate for this zone of the considered frequency range.

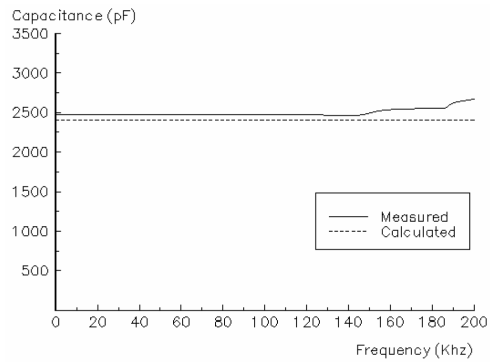

Fig. 5. Measured and calculated capacitance

3. Time Domain Winding Model

In reference (3), a three phase computer model for calculating the terminal impedance of machine windings in the frequency domain has been presented by the authors. The accuracy of this Frequency Domain Machine Winding (FDMW) model is shown in Figure 6, where a comparison of the terminal impedance measured and calculated is presented. The aim of this paper is to obtain terminal models for this impedance and use it in transient overvoltage calculations. The following sections describe two methods of synthesis.

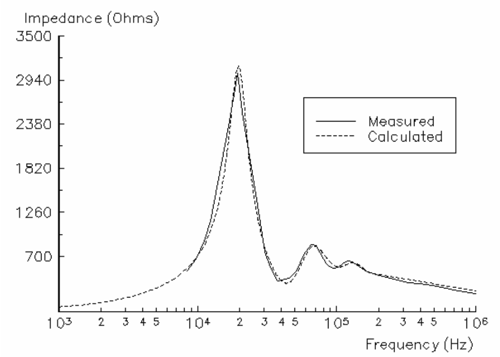

Fig. 6. Terminal impedance measured and calculated.

3.1. Minima resonance method (MIRM).

This method is useful for calculating a series RLC branch for each minima resonant frequency of the winding impedance [7]. For an impedance with three minima (m=3) and two maxima (n=2) resonant frequencies the equivalent circuit has three series RLC branches in parallel, as shown in Figure 7.

From the admittance equation for the whole network, not taking into account the resistors, the value of the inductors can be calculated by [7]:

$$\begin{bmatrix} 1 & 1 & 1 \\ \omega_2^2+\omega_3^2 & \omega_1^2+\omega_3^2 & \omega_2^2+\omega_1^2 \\ \omega_2^2\omega_3^2 & \omega_1^2\omega_3^2 & \omega_2^2\omega_1^2 \end{bmatrix} \begin{bmatrix} 1/L_1 \\ 1/L_2 \\ 1/L_3 \end{bmatrix} = \begin{bmatrix} 1 \\ W_1^2+W_2^2 \\ W_1^2 W_2^2 \end{bmatrix} \qquad (8)$$

where $T_{j,\ j=1,2,3}$ represents the minima resonance frequencies and $W_{i,\ i=1,2}$ are the maxima resonance frequencies.

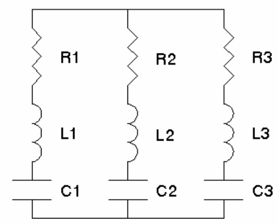

Fig. 7. Equivalent circuit with three RLC branches.

Once the inductances are calculated, the values of the capacitors are computed using:

$$\omega_j^2 = \frac{1}{L_j C_j} \qquad j = 1,2,3 \qquad (9)$$

The network of m LC branches obtained from the solution of (8) y (9) has zero impedance (resistance) at minima resonance frequencies and infinite impedance (resistance) at maxima resonance frequencies. In order that the minima points of the network impedance becomes similar to those of the winding impedance it is necessary to insert the m resistances with values equal to the magnitude of the winding impedance at the minima resonance points. However, this would still leave maxima resonance points of the equivalent circuit much larger than those of the winding impedance. Correction of this error requires scaling of all inductors and capacitors: the scaling factor would be the same for all inductors and capacitors, so that the resonance frequencies remain the same. The scaling factor is given by:

$$SF = \frac{Z_{ec}}{Z_m} \qquad (10)$$

where Z_{ec} is the magnitude of the equivalent circuit impedance and Z_m is the magnitude of the winding impedance. The appropriate scaling factor can be obtained by calculating the impedances at a particular frequency at which best match is required. All inductors in the equivalent circuit are multiplied and all capacitors are divided by this factor.

3.2. Maxima Resonance Method (MARM)

This method is described in [8] and it is used to obtain a RLC block for each maxima resonant frequency. Figure 8 shows the equivalent circuit of the winding impedance for the i-th resonance frequency.

The real and imaginary part of the equivalent circuit impedance are:

$$Z_{real} = \frac{R_{pi}R_{si}^2 + R_{pi}^2 R_{si} + \omega_i^2 R_{pi} L_i^2}{[R_{pi} + R_{si} - \omega_i^2 R_{pi} L_i C_i]^2 + [\omega_i L_i + \omega_i R_{pi} R_{si} C_i]^2} \qquad (11)$$

$$Z_{imag} = \frac{\omega_i R_{pi}^2 L_i - \omega_i^3 R_{pi}^2 L_i^2 C_i - \omega_i R_{pi}^2 R_{si}^2 C_i}{[R_{pi} + R_{si} - \omega_i^2 R_{pi} L_i C_i]^2 + [\omega_i L_i + \omega_i R_{pi} R_{si} C_i]^2} \qquad (12)$$

Equations (11) and (12) are non-linear and contains 4 unknowns: R_{pi}, R_{si}, L_i and C_i. The series connection of n circuits can be used to represent winding impedance with n maxima resonance frequencies. The network impedance function has 4*n unknown parameters, which can be calculated taking 2*n values of the impedance at different frequencies, including the maxima resonance points. The result is a total of 4*n nonlinear equations which can be solved with Newton method.

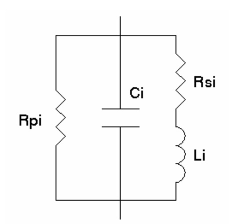

Fig. 8. Equivalent circuit for the i-th resonant frequency.

4. Results and Discussions.

Computer simulations were carried out considering a phase winding of the electrical motor under study.

4.1 Short Circuit Conditions.

Two electrical circuits are calculated using the methods of synthesis for the terminal impedance obtained with the FDMW model. The networks are simulated using the Alternative Transients Program (ATP).

Figure 10 shows the terminal impedances calculated with FDMW, MIRM and MARM models. From this figure it can be seen that the methods of synthesis have a reasonably degree of accuracy since magnitude is moderately well reproduced and general features of the frequency variation are common to FDMW and both equivalent circuits. Also, it is observed that the MARM technique has a better accuracy than the MIRM, especially at the main resonant frequency.

The voltages measured and calculated at winding terminals are presented in Figure 11. From this, it is clear that the equivalent circuits are useful for calculating with good accuracy the transient behavior of the winding. Again, it can be observed that the equivalent circuit obtained with MARM gives better results than those simulated with the network computed with MIRM.

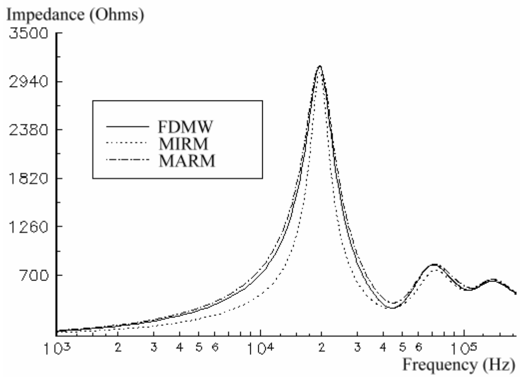

Fig. 10 Terminal impedances calculated with several models and machine winding grounded.

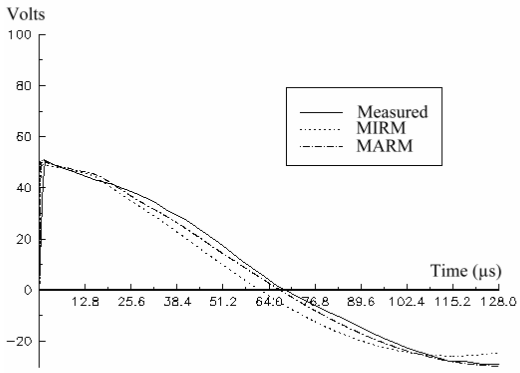

Fig. 11. Voltages measured and calculated for the winding grounded.

4.2 Open Circuit Conditions.

From the previous results, it has been concluded that the MARM has better accuracy than the MIRM; so the MARM is used for calculating the equivalent circuit for the winding with its end terminal floating. In this case, the impedance is capacitive at low frequencies, so an additional capacitor is included in the equivalent circuit. The equation related to this capacitor is added to (12), which leads to an over-determined nonlinear system of equations whose solution can be obtained using nonlinear least squares estimation.

The impedances calculated with FDMW and MARM are presented in Figure 12. Again, it can be seen that the two impedances have similar magnitude and features in the frequency variation.

The transient voltage computed with FDMW and MARM are presented in Figures 13 and 14, respectively. In both figures it can be observed that the voltage surges have similar magnitudes and propagation times, leading to the conclusion that the equivalent circuit in the time domain is valid for calculating the transient response of the machine winding.

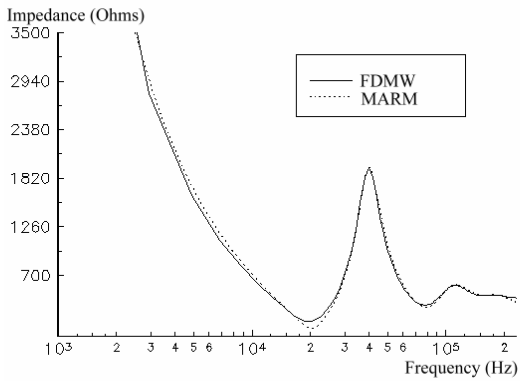

Fig. 12 Terminal impedances calculated with several models and the winding floated.

5. Conclusions.

A full procedure for modeling rotating machine windings for switching transient studies has been presented. The terminal models were developed using network synthesis for the winding impedance. The equivalent circuits were obtained with two methods:

The first one considers mainly minima resonance points and the second is based on maxima resonance frequencies. The networks were simulated with ATP.

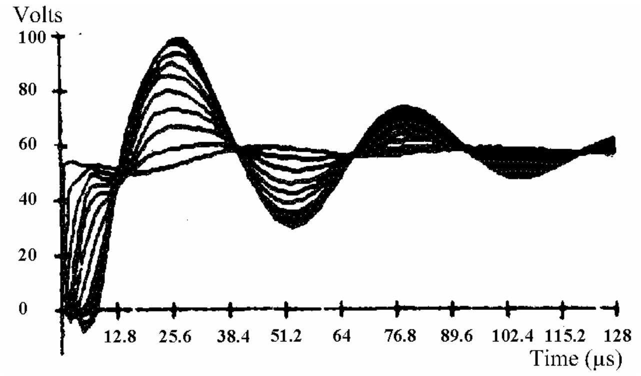

Fig. 13 Voltage measured for the winding floated.

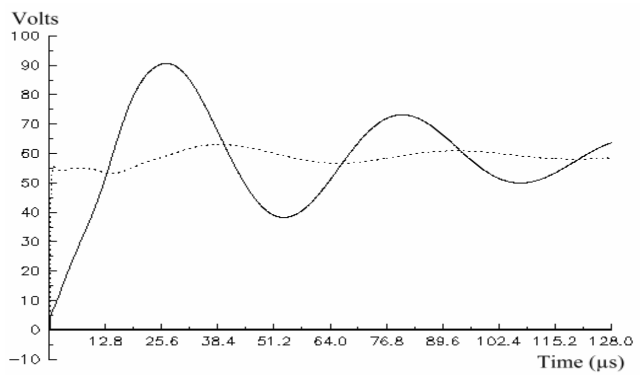

Fig. 14 Voltage calculated with MARM for the winding floated.

The computer results calculated with the equivalent circuits were compared with simulations made with a transmission line model in the frequency domain. The comparison shows that the network models are accurate for calculating winding impedance and voltage transients.

The results obtained are useful in the development of three-phase models for studying switching surges due to the second and third pole closure in industrial installations.

References

[1] W.L. Keerthipala and P.G. McLaren, “A multiconductor transmission line model for surge propagation studies in large AC machine windings”, Paper CH2819-1/90/0000-0629, 1991 IEEE.

[2] J.L. Guardado and K.J. Cornick, "A computer model for calculating steep fronted surge distribution in machine windings," IEEE Trans. EC, Vol. 4, No. 1, March 1989.

[3] J.L. Guardado, K.J. Cornick, V. Venegas, J.L. Naredo, E. Melgoza, "A three-phase model for surge distribution studies in electrical machines", Paper 96 SM 365-7 EC, IEEE/PES Summer Meeting, July 1996.

[4] K.J. Cornick and T.R. Thompson, "Steep fronted switching voltage transients and their distribution in motor windings. Part 1: System measurements of steep-fronted switching voltage transients," Proc. IEE, Vol. 129. Pt. B, p.45-55, March 1982.

[5] K.J. Cornick and T.R. Thompson, “Steep-fronted switching voltage transients and their distribution in motor windings. Part 2: Distribution of steep fronted switching voltage transients in motor windings,” Proc IEE, Vol. 129, Pt. B. No.2, March 1982.

[6] P.J. Lawrenson, “Calculation of machine end-winding inductances with special references to turbogenerators”, Proc. IEE, Vol. 117, No. 6, June 1970.

[7] N.G. Hingorani and M.F. Burbery, “Simulation of AC system impedance in HVDC System Studies”, IEEE/PAS, Vol. PAS-89, No. 5/6, May/June 1970.

[8] I.A. Metwally, “Simulation of the impulse response of electrical machines”, IEEE/EC, Vol. 14, No. 4, December 1999.